Yrast structure of ^{206}Bi: Isomeric states and one-proton-particle, three-neutron-hole excitations

N. Cieplicka,[1] K. H. Maier,[1] B. Fornal,[1] B. Szpak,[1] R. V. F. Janssens,[2] M. Alcorta,[2] R. Broda,[1] M. P. Carpenter,[2] C. J. Chiara,[2,3] C. R. Hoffman,[2] B. P. Kay,[2,*] F. G. Kondev,[2] W. Królas,[1] T. Lauritsen,[2] C. J. Lister,[2] E. A. McCutchan,[2,†] T. Pawłat,[1] A. M. Rogers,[2] D. Seweryniak,[2] N. Sharp,[3] W. B. Walters,[3] J. Wrzesiński,[1] and S. Zhu[2]

[1]*Institute of Nuclear Physics, Polish Academy of Sciences, PL-31342 Kraków, Poland*

[2]*Physics Division, Argonne National Laboratory, Argonne, Illinois 60439, USA*

[3]*Department of Chemistry and Biochemistry, University of Maryland, College Park, Maryland 20742, USA*

(Received 14 July 2012; published 29 November 2012)

New high-spin microsecond isomers, with $J^\pi = (31^+)$ and $J^\pi = (28^-)$, have been identified in ^{206}Bi at 10 170 and 9233 keV, respectively, using γ-ray coincidence spectroscopy following deep-inelastic reactions with the ^{76}Ge + ^{208}Pb system. Yrast and near-yrast levels populated in the decay of these isomers have been located and interpreted with the help of shell-model calculations. The states identified at energies up to approximately 7 MeV can be described well in terms of one-proton-particle, three-neutron-hole couplings.

DOI: 10.1103/PhysRevC.86.054322 PACS number(s): 23.20.Lv, 27.80.+w, 23.20.En, 21.60.Cs

I. INTRODUCTION

As ^{208}Pb is considered to be one of the best doubly-magic nuclei, the region surrounding this nucleus is a favorable testing ground for modern shell-model calculations. The nucleus ^{206}Bi, the subject of the present work, belongs to this region. Of particular interest in this nuclide are high-spin yrast states. Such excitations often arise from the maximum spin coupling of the valence particles/holes and are usually rather pure, because their wave functions involve mostly one well-defined configuration. These states are well suited for comparisons between experiment and theory because their excitation energies can be calculated by using only a small number of diagonal two-body matrix elements.

The ^{206}Bi nucleus is a one-proton-particle, three-neutron-hole (1p-3h) system with respect to the doubly-magic ^{208}Pb core. Its low-energy yrast and near yrast structure arises primarily from 1p-3h couplings involving $1h_{9/2}$, $2f_{7/2}$, and $1i_{13/2}$ proton particles, and $3p_{1/2}$, $2f_{5/2}$, $3p_{3/2}$, $2f_{7/2}$, $1h_{9/2}$, and $1i_{13/2}$ neutron holes. The ^{206}Bi ground state, with spin-parity $J^\pi = 6^+$, is of $\pi h_{9/2}\nu f_{5/2}^{-1}$ character, with the isomeric ($T_{1/2} = 7.7\ \mu$s) $J^\pi = 4^+$ member of the $\pi h_{9/2}\nu p_{1/2}^{-1}$ multiplet lying only 60 keV above it. At higher excitation energies, two other isomeric states have been identified in an earlier study with the ^{205}Tl(α,3nγ) reaction [1]. These are the 10^- state at 1045 keV, with $T_{1/2} = 0.89$ ms and an assigned $(\pi h_{9/2}\nu i_{13/2}^{-1}) \times \nu_0^{-2}$ configuration, and the 15^+ excitation of $\pi h_{9/2}\nu p_{1/2}^{-1} i_{13/2}^{-2}$ character located at 3147 keV, with a 15.6-ns half-life. The highest ^{206}Bi yrast states known thus far, i.e., the 17^+ and 18^+ levels at 3604 and 4305 keV, have been located in the ^{205}Tl(α,3nγ) work as well [1].

States with higher spin, which can be explained as arising from the coupling of the valence proton particle and three neutron holes, are expected to occur in the energy range up to about 7 MeV. The highest spin and parity available as a result of such a coupling is 23^+ and originates from a configuration with the proton particle and three neutron holes all occupying the $1i_{13/2}$ orbital. Above 7 MeV, the ^{206}Bi yrast level structure should become more complex as higher-lying states have to involve core excitations, that is, the promotion of neutrons or protons across the $N = 126$ or $Z = 82$ energy gaps, respectively. These high-lying states in ^{206}Bi could not be reached in previous studies such as with the ^{205}Tl(α,3nγ) reaction of Ref. [1].

A successful method for investigating the high-spin yrast structure of nuclei around ^{208}Pb uses deep-inelastic reactions [2–6] occurring during heavy-ion collisions at beam energies around 20% above the Coulomb barrier. In such deep-inelastic processes, the production yield is spread over many nuclei, but, owing to the high resolving power of modern, large detector arrays, the extraction of detailed information from coincidence data sets with large statistics, even for weak reaction channels, is possible [7].

In the present work, high-spin states in ^{206}Bi were populated in deep-inelastic collisions induced by a ^{76}Ge beam on a ^{208}Pb target. An extensive γ-ray coincidence measurement was carried out with the Gammasphere multidetector array [8]. As a result, additional yrast and near-yrast levels in ^{206}Bi were established, extending up to about 10 MeV. Two new isomeric states were located: one at about 9 MeV and the second, long-lived, lying at an excitation energy of ~10 MeV. An interpretation of the ^{206}Bi level structure above the 10^- isomer is presented. For the levels arising from couplings of the valence particle and holes, the ^{206}Bi nucleus offers the potential of instructive comparisons with shell-model calculations: this is also discussed. Spin-parity assignments to the newly identified states up to $J^\pi = 23^+$ are presented, based on their decay pattern and comparisons with theory. For the levels resulting from core excitations, angular distributions of γ rays together with extracted conversion coefficients provide information about transition multipolarities as well as firm, relative spin and parity assignments.

*Present address: Department of Physics, University of York, Heslington, York YO10 5DD, UK.

†Present address: National Nuclear Data Center, Brookhaven National Laboratory, Upton, New York 11973-5000, USA.

II. EXPERIMENTAL PROCEDURE AND RESULTS

A. Construction of the level scheme

The experiment was performed at Argonne National Laboratory with a ^{76}Ge beam from the Argonne Tandem Linear Accelerator System (ATLAS) and the Gammasphere array [8], which consisted of 101 Compton-suppressed Ge detectors. The 450-MeV beam was focused on a 56 mg/cm^2 ^{208}Pb target, placed in the center of the spectrometer. Coincidence data were collected with an event trigger requiring three or more Compton-suppressed γ rays to be measured in coincidence within a 2-μs time window. The trigger signal was correlated in time with the first coincident γ ray. Each event contained energy and timing information for all Ge detectors that fired within 1.3 μs of the trigger signal. A total of 2.1×10^9 three- and higher-fold events were recorded. The beam, coming in bursts with a ∼0.3-ns time width, was pulsed with a 412-ns repetition rate in order to provide clean separation between prompt and isomeric events. Conditions set on the $\gamma\gamma$ time parameter were used to obtain various versions of prompt and delayed $\gamma\gamma$ and $\gamma\gamma\gamma$ coincidence histograms covering γ-ray energy ranges up to ∼4 MeV.

The ^{206}Bi decay scheme established in previous studies [1] is printed in black and white in Fig. 1. In this earlier scheme, the highest yrast excitation is the 18^+ state at 4307 keV decaying via a cascade of a few γ rays that feed the 10^-, 0.89-ms isomer at 1045 keV. The analysis of the data from the present experiment fully confirmed this 18^+ level and transition assignments. Hence, this information was subsequently used as a starting point for the delineation of higher yrast excitations. In a first step, double coincidence gates were placed in the off-beam cube on various pairs of known transitions at 701, 458, 505, 543, 548, 266, 744, 150, and 595 keV. Many off-beam coincidence spectra produced in this way—see Fig. 2 for representative examples—were investigated and provided clean evidence for new transitions belonging to ^{206}Bi which, apparently, followed the decay of unknown higher-lying isomers.

As a first step in the analysis, a cascade was identified consisting of 1152-, 189-, 214-, 304-, and 417-keV γ rays feeding the first 16^+ state at 3652 keV. The ordering of these transitions was established based on their intensities and the presence of parallel decay branches such as the 1234-, 1371-, and 1388-keV lines. This first step provided the location of new levels at 4805, 4993, 5207, 5511, and 5928 keV. Further, the first 18^+ state at 4307 keV was found to be populated by a sequence of 1485-, 1102-, and 231-keV transitions which identify additional new levels at 5793, 6895, and 7126 keV. The location of the highest of these excitations at 7126 keV was confirmed by the presence of yet another cascade of 777-, 467-, 503-, and 1772-keV γ rays connecting it to the lower portion of the scheme via new states at 6349, 5882, and 5378 keV. Further support for the proposed level arrangement came from the analysis of weaker transitions found only by summing the appropriate coincidence spectra. For example, levels placed at 4982, 5096, and 5278 keV were found to be fed by the 1913-231-keV, 513-332-1074-111-keV, and 124-110-1234-245-136-keV cascades, respectively. Some of the low-energy transitions at 110, 111, 118, 124, 136, and 245 keV were observed only as weak peaks, even in the summed spectra, most likely because of strong internal conversion. Furthermore, an addition is proposed to the structure in the known part of the scheme as a 2951-keV level was defined by the 196-1162-keV cascade and confirmed through a 451-keV decay branch.

While performing the γ-coincidence analysis described above, a set of five intense, mutually coincident γ rays with energies of 361, 480, 553, 713, and 937 keV was found to be present in all spectra. After the construction of a consistent level scheme up to the 7126-keV level, it became clear that this new cascade originates above this state. In addition, because all these new lines appeared in the off-beam spectra, it became apparent that they have to belong to a cascade deexciting one or more new high-lying isomers. This strong cascade was, therefore, placed at the top of the level scheme of Fig. 1. The ordering of the 361-, 480-, 553-, 713-, and 937-keV γ rays was determined based on the analysis of the transition intensities measured in both the in- and off-beam spectra (the ratio of prompt to delayed intensities has to decrease monotonically with excitation energy, independently of branching and detector efficiency; see Table I). This part of the analysis established new levels at 7679, 8159, 8520, 9233, and 10 170 keV above the 7126-keV excitation.

It was noticed by double gating on the 553-, 480-,361-, and 713-keV lines in the prompt-delayed-delayed cube that the 937-keV transition is clearly visible and must be preceding in time this cascade. This observation pointed to the existence of yet another isomeric state at 9233 keV decaying via the 713-keV line. Gates placed on various combinations of the 744-, 595-, 266-, 548-, 543-, 458-, and 701-keV γ rays displayed also other transitions belonging to the structure above the 7126 keV-state. These were the 477-keV line (parallel to the 553-keV γ ray) and a cascade consisting of 346- and 568-keV transitions which connects the 8159- and 7202-keV levels. From the differences in energies of the levels, the existence of two unobserved, low-energy transitions (76 and 43 keV for the 477-keV transition and 346-568-keV cascade, respectively) was inferred. Their placement is tentative and is also discussed in Sec. III. The connection of the 8159- and 7126-keV levels by a 346-568-119-keV cascade was excluded because a required 119-keV transition was not present in the spectra.

The intensities of the identified γ rays were obtained from double-gated coincidence spectra in the off-beam data. At first, the intensities of the 744-, 595-, and 150-keV transitions at the bottom of the scheme were established relative to each other from the spectrum gated on the 266- and 548-keV lines. The next step was to calculate the intensities of the 815-, 548-, 1162-, and 711-keV γ rays from the 595-713-keV gated spectrum assuming that their sum is equal to the sum of intensities measured for the 744- and 595-keV transitions. The intensities of stronger lines were calculated relative to the 548-keV line from the same spectrum. In the case of weaker transitions, the intensities were obtained from the sum spectra, for example, in the spectrum gated on every pair among the 361-, 595-, 713-keV transitions, the intensities of lines such as those at 1906, 1913, 2581, 2587, and 2683 keV were calculated relative to the 458-keV yield. The intensity of the 713-keV line was obtained from the 266-361-keV gated spectrum, relative to

TABLE I. Information on levels and transitions in ^{206}Bi from the present experiment.

E_{ini} (keV)	J^{π}_{ini}	E_{fin} (keV)	J^{π}_{fin}	E_{γ} (keV)	$I_{delayed}$	I_{prompt}	Ratio $\left(\frac{I_{prompt}}{I_{delayed}}\right)$
1639	11^-	1045	10^-	594.8(1)[a]	71(4)	71(2)	1.00(7)
1789	12^-	1639	11^-	149.8(1)[a]	24(4)	23(1)	0.94(17)
		1045	10^-	744.5(1)[a]	32(2)	31(1)	0.99(9)
2056	13^-	1789	12^-	266.4(1)[a]	61(5)	63(7)	1.04(14)
2500	13^-	1789	12^-	711.0(1)[a]	12(2)	12(3)	1.00(31)
2604	14^-	2056	13^-	548.1(1)[a]	73(5)	73(7)	0.99(11)
		1789	12^-	814.8(1)	8(1)	7(1)	0.89(20)
2951	(14^-)	2500	13^-	451.2(1)	12(2)	12(3)	0.99(31)
		1789	12^-	1161.8(2)	9(2)	8(1)	0.93(27)
3147	15^+	2951	(14^-)	196.0(1)	21(2)	16(3)	0.79(15)
		2604	14^-	543.5(1)[a]	84(7)	80(7)	0.96(12)
3606	17^+	3147	15^+	458.4(1)[a]	79(7)	54(6)	0.68(9)
3652	16^+	3147	15^+	505.1(1)[a]	25(2)	15(3)	0.59(13)
4307	18^+	3606	17^+	701.5(1)[a]	48(6)	20(4)	0.41(9)
4687	(16^-)	2951	(14^-)	1735.7(3)	5(1)	[b]	
		2604	14^-	2083.4(2)	2(1)	[b]	
4775	(16^-)	3652	16^+	1121.9(1)	5(1)	2(1)	0.34(13)
4805	(17^-)	4775	(16^-)	(30)	[b]	[b]	
		4687	(16^-)	118.5(4)	<1	[b]	
		3652	16^+	1152.4(2)	11(2)	8(2)	0.74(22)
4982	(19^+)	4307	18^+	674.5(1)	14(2)	2(1)	0.18(6)
4993	(18^-)	4805	(17^-)	188.6(2)	13(4)	5(1)	0.35(12)
		3606	17^+	1387.9(1)	5(1)	4(1)	0.78(27)
5096	(18^-)	4805	(17^-)	292.0(1)	9(1)	2(1)	0.26(8)
		4307	18^+	788.9(2)	12(3)	6(2)	0.52(19)
5207	(19^-)	4993	(18^-)	213.7(2)	16(4)	6(2)	0.39(14)
5278	(18^-)	4307	18^+	970.4(2)	11(2)	4(1)	0.39(11)
5378	(18^-)	3606	17^+	1772.2(2)	8(2)	6(1)	0.81(24)
5402	(19^-)	5278	(18^-)	124	[b]	[b]	
5511	(20^-)	5402	(19^-)	110	[b]	[b]	
		5207	(19^-)	304.3(2)	13(1)	5(1)	0.39(9)
5610	(19^-)	5096	(18^-)	513.1(1)	14(1)	10(2)	0.69(17)
5793	(19^-)	4307	18^+	1485.4(2)	7(1)	2(1)	0.23(8)
5882	(19^-)	5378	(18^-)	503.4(1)	4(1)	3(2)	0.80(51)
5928	(21^-)	5511	(20^-)	417.0(3)	15(3)	3(1)	0.20(7)
5941	(20^-)	5610	(19^-)	331.6(4)	5(1)	[b]	
6349	(20^-)	5882	(19^-)	466.8(5)	<1	[b]	
6578	(19^+)	5207	(19^-)	1370.7(5)	3(2)	2(1)	0.48(38)
6745	(19^+)	6578	(19^+)	166.6(2)	3(1)	[b]	
		5511	(20^-)	1234.5(2)	3(1)	[b]	
6888	(20^+)	5610	(19^-)	1277.9(5)	2(1)	[b]	
		4982	(19^+)	1906.2(2)	2(1)	[b]	
		4307	18^+	2580.8(3)	<1	[b]	
6895	(20^+)	5793	(19^-)	1102.0(1)	10(2)	0.6(2)	0.06(2)
		4982	(19^+)	1913.4(2)	3(1)	[b]	
		4307	18^+	2586.6(4)	2(1)	[b]	
6990	(20^+)	6745	(19^+)	245	[b]	[b]	
		5941	(20^-)	1049.0(2)	2(1)	[b]	
		5928	(21^-)	1059.7(2)	2(1)	[b]	
		4307	18^+	2683.3(4)	3(1)	0.6(2)	0.23(11)
7015	(21^+)	5941	(20^-)	1073.8(2)	4(1)	[b]	
		5928	(21^-)	1085.2(1)	2(1)	[b]	
7126	(22^+)	7015	(21^+)	111	[b]	[b]	
		6990	(20^+)	136	[b]	[b]	
		6895	(20^+)	230.8(2)	17(3)	1.4(3)	0.08(3)
		6888	(20^+)	237.5(2)	8(2)	[b]	
		6349	(20^-)	777.3(2)	<1	[b]	

TABLE I. (*Continued.*)

E_{ini} (keV)	J^{π}_{ini}	E_{fin} (keV)	J^{π}_{fin}	E_{γ} (keV)	$I_{delayed}$	I_{prompt}	Ratio $\left(\frac{I_{prompt}}{I_{delayed}}\right)$
7202	(23^+)	7126	(22^+)	(76)	[b]	[b]	
7679	(24^+)	7202	(23^+)	477.4(1)	8(1)	1(0.5)	0.08(3)
		7126	(22^+)	552.9(1)	71(10)	7(1)	0.10(3)
7770	?	7202	(23^+)	568.3(2)	19(4)	3(1)	0.14(4)
8116	?	7770	?	346.4(2)	16(3)	2(1)	0.12(4)
8159	(25^+)	8116	?	(43)	[b]	[b]	
		7679	(24^+)	480.2(1)	69(6)	5(1)	0.08(2)
8520	(26^+)	8159	(25^+)	361.2(1)	79(10)	6(1)	0.07(2)
9233	(28^-)	8520	(26^+)	713.2(1)	91(5)	4(1)	0.04(1)
10170	(31^+)	9233	(28^-)	937.2(1)	31(5)	0	0

[a] γ rays seen also in Ref. [1].
[b] Intensity too weak to be determined.

the 543-keV transition. All the intensities were normalized to that of the 713-keV line (after the inclusion of the contribution from internal conversion, its intensity was defined as 100). A similar analysis was made for the prompt transitions assuming that the prompt/delayed intensity ratio for the 595-keV line deexciting the lowest observed level (1639 keV) is equal to 1.

The delayed intensity of the higher, strong transition at 713 or 361 keV is equal to the sum of the yields for the 744- and 595-keV γ rays. However, in the medium part of the scheme, below the 7126-keV level, up to 74% of the intensity is missing. This observation indicates that (a) many decay branches remain unobserved, due to their weak intensity and (b) the level structure in this region is even more complex than deduced in the present study.

A detailed analysis of the intensity balance for the lines above the 7126-keV level was performed to obtain information on the total conversion coefficients of some of the transitions of interest. For example, the coefficient for the 361-keV line, 0.26(2), was obtained by comparing its intensity to the sum of the intensities of the 477- and 553-keV transitions (the strong 553-keV γ ray is an $E2$ transition and has a small conversion coefficient) in the spectrum gated on pairs of lines with the 480-keV γ ray and any of the 266-, 458-, 543-, 701-, 744-keV transitions. A similar analysis carried out for the 480-, 553-, and 713-keV γ rays resulted in the determination of their conversion coefficients as well (Table II).

As stated above, the 9233-keV level is an isomer fed by a 937-keV transition. Its half-life could then be determined from a spectrum of time differences between the detection time of the 937-keV γ ray with respect to the 361-, 458-, and 480-keV transitions that deexcite the isomer. The analysis yielded $T_{1/2} = 155(15)$ ns (Fig. 3). In addition, the 937-keV line deexcites a level at 10 170 keV, which is also an isomer. To estimate $T_{1/2}$ for this long-lived state, a time spectrum started by the rf signal of the accelerator and stopped by the detection of the 937-keV transition was constructed while requiring in addition a coincidence between this line and other strong γ rays in the decay cascade (Fig. 1). In the electronics setup used here, this spectrum covers effectively only a 400-ns range, which was sufficient only to establish that the associated $T_{1/2}$ value must be larger than 2 μs.

The information on all the transitions and energy levels deduced in the present work is summarized in Table I.

TABLE II. Total conversion coefficients $\alpha_{tot-exp}$, angular-distributions coefficients A_2 and A_4, and mixing ratios δ. The second column gives the measured delayed intensity, while the third provides the total intensity as expected from the decay scheme. Specific set of gates was applied to reduce the intensity uncertainties. Column 4 presents the deduced from the missing γ-ray intensities total conversion coefficient and column 5 the theoretical value for the assigned multipolarity. The last three columns provide the measured angular-distribution coefficients and the ensuing mixing ratios.

E_{γ} (keV)	I_{γ}	I_{tot}	$\alpha_{tot-exp}$	$\alpha_{tot-theor}$	A_2	A_4	δ
118	0.8(4)	7.0(3)	8(4)	6.35($M1$)	–	–	–
361	79.4(11)	100.0(12)	0.26(2)	0.28($M1$)	−0.14(1)	−0.01(2)	−0.08(2)
458					0.21(6)	−0.03(8)	0.0
480	68.6(11)	81.0(14)	0.18(4)	0.13($M1$)	−0.22(5)	0.06(7)	−0.20(9)
543					−0.18(4)	−0.02(5)	0.0
548					−0.33(3)	0.02(4)	−0.14(3)
553	70.9(12)	73.0(16)	0.03(4)	0.02($E2$)	0.13(1)	−0.05(1)	0.0
701					−0.34(5)	0.00(6)	−0.15(5)
713	90.9(13)	100.0(13)	0.10(3)	0.12($M2$)	0.14(2)	0.00(3)	0.03(5)

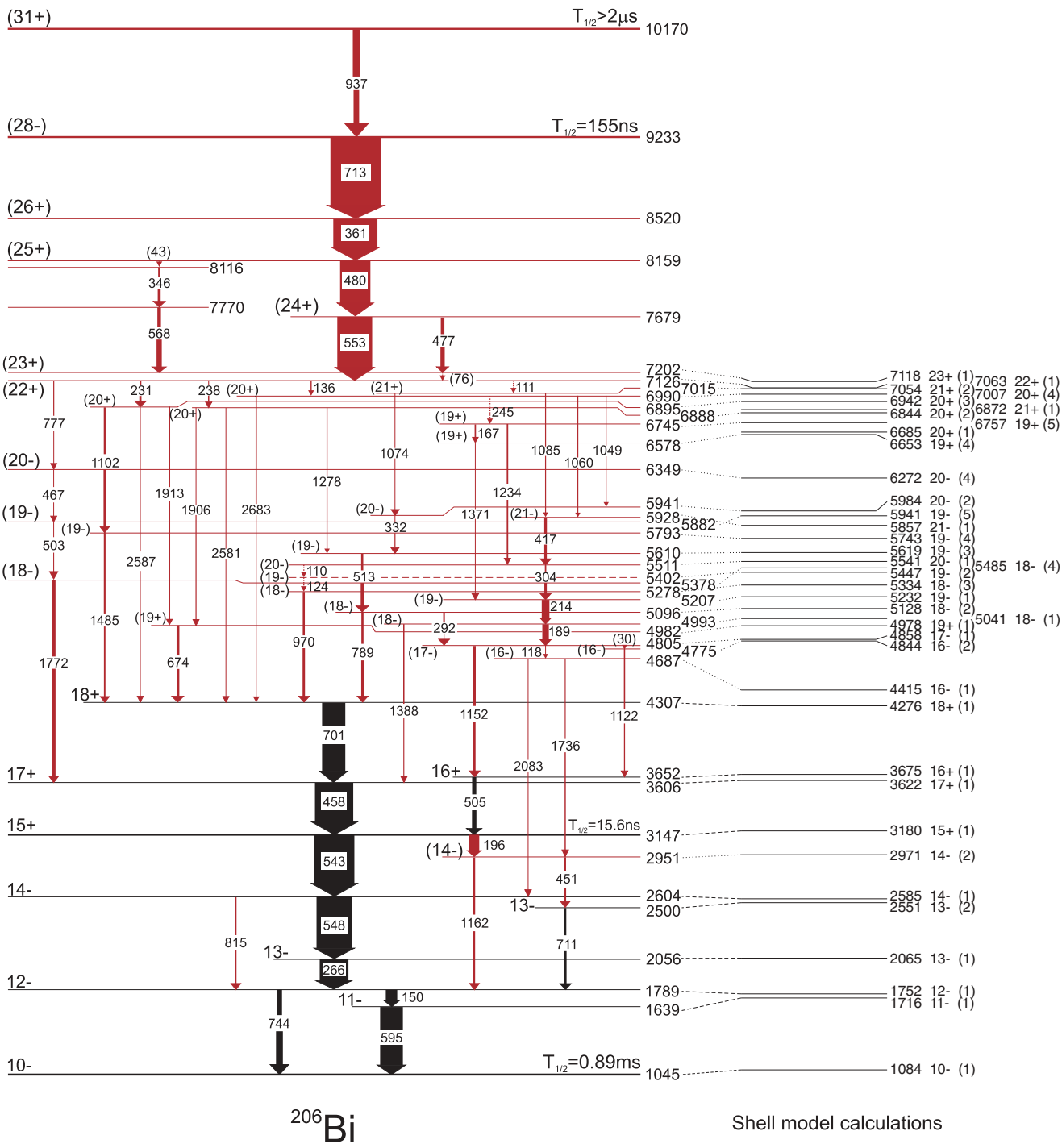

FIG. 1. (Color online) Proposed level scheme for the high-spin states in ^{206}Bi (left) compared with the results of shell-model calculations (right). Transitions in red were identified in the present study. Intensities are indicated by the widths of the arrows. The energies are not excitation energies, but rather binding energies relative to ^{208}Pb, but shifted by -18.645 MeV so that the experimental ground state of ^{206}Bi is at 0. Note that the low-spin level structure of ^{206}Bi is not shown, but can be found in Ref. [9]. Note that there is uncertainty of $1\hbar$ for the spin assignments to the levels located above the 7202-keV state; see text for a detailed discussion.

B. Angular distributions and multipolarity determinations

As mentioned earlier, the yrast cascade above the long-lived 10^- isomer extending up to an 18^+ level was established and the spin-parity of the states determined with the help of γ-ray angular distributions following the ^{205}Tl$(\alpha,3n\gamma)^{206}$Bi reaction by Lönnroth *et al.* [1]. The question arose as to whether the levels populated in the ^{76}Ge + ^{208}Pb experiment exhibit sufficient spin alignment to use γ-ray angular distributions for multipolarity assignments. To check this possibility, the angular distributions for low-lying, intense γ

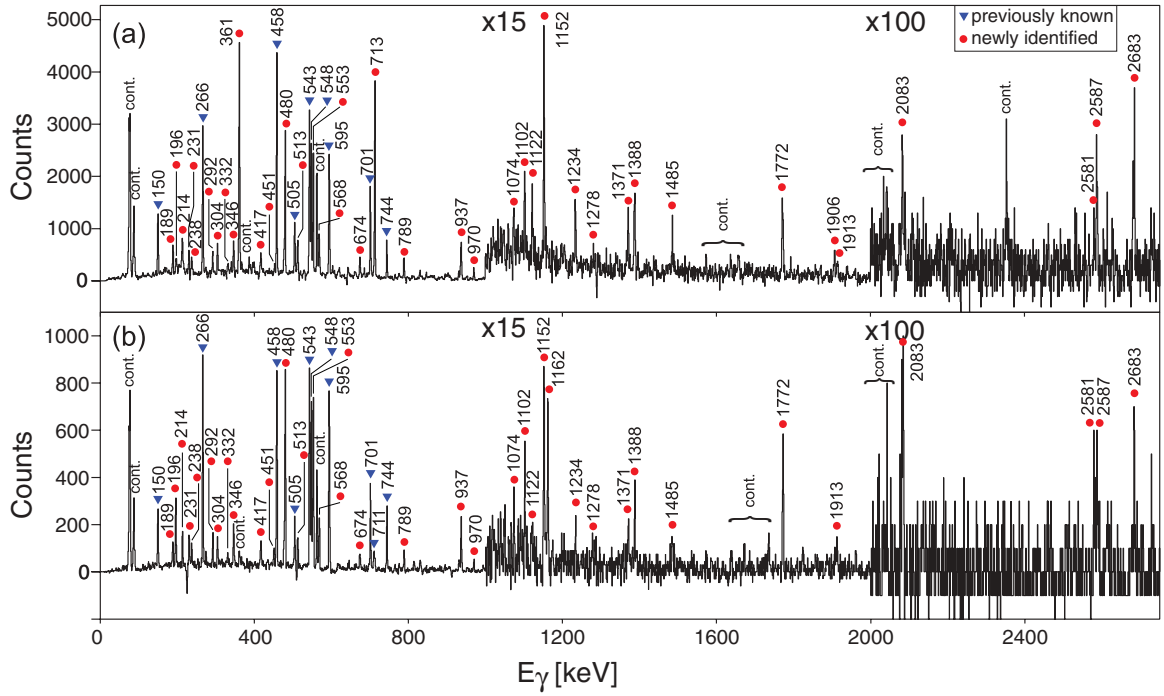

FIG. 2. (Color online) Representative off-beam coincidence spectra. (a) Sum spectrum double gated on every pair of transitions at 150, 266, 543, 548, and 595 keV; (b) spectrum gated on the 361- and 713-keV transitions.

rays in ^{206}Bi were first investigated by applying the following procedure.

The Gammasphere detectors were grouped into six rings around the beam axis with the following average values of the angle θ: 17.3°, 35.5°, 52.8°, 69.8°, 79.9°, 90.0°. Their equivalents for backward angles rings were available as well. The intensities of the lines observed in these rings can be used to construct the angular distributions of the γ rays. A cube was constructed for each ring from prompt triple coincidence events. The γ rays detected in a specific ring were allocated to one axis and the two other coincident photons from any detector in other rings to the other two axes. Spectra for the rings were then generated by double gating on any pair of the 361-, 480-, 553-, 970-, 701-, 458-, 543-, 548-, 266-, and 744-keV lines. The counts in various rings were normalized using the isotropic distribution of the 516-881-803-keV cascade deexciting the 125-μs isomer in ^{206}Pb [9]. Sample angular distributions obtained in this way are presented in Fig. 4.

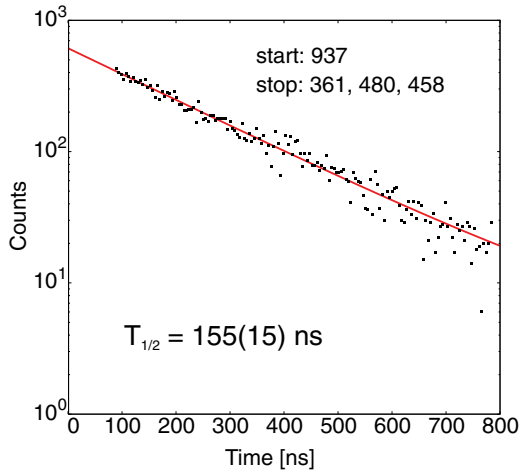

FIG. 3. (Color online) Summed time distribution between the 937-keV γ ray and any of the 361-, 480-, or 458-keV lines.

As the direction of the products of deep inelastic reactions are not measured in a thick target experiment, the only definite axis in the laboratory is the beam direction. This is the same situation as in fusion-evaporation reactions and the familiar formalism for the angular distributions can be applied [10,11]. The angular distribution is parametrized by the two coefficients A_2 and A_4 of the Legendre polynomials $P_n(\cos\theta)$ in

$$W(\theta) = A_0[1 + A_2 P_2(\cos\theta) + A_4 P_4(\cos\theta)].$$

These coefficients depend on the angular momentum alignment of the nucleus resulting from the reaction, the spins of the two levels involved in the γ decay, as well as on the multipolarity and mixing ratio of the transition. For lack of more detailed information, the occupation of the m-states of the nucleus is usually described by a Gaussian distribution. The width of this distribution is the single free parameter determining the alignment, and it can be extracted from the attenuation of the A_2 coefficient determined for a known transition. This then also determines the attenuation of the A_4 coefficient.

The 458-keV ($17^+ \rightarrow 15^+$) transition is of pure $E2$ character, while the 543-keV ($15^+ \rightarrow 14^-$) γ ray is a pure $E1$ transition. The attenuation of the former transition was measured to be 0.54(15) and agrees with that inferred from the latter of 0.64(14). The attenuation of the A_2 coefficient

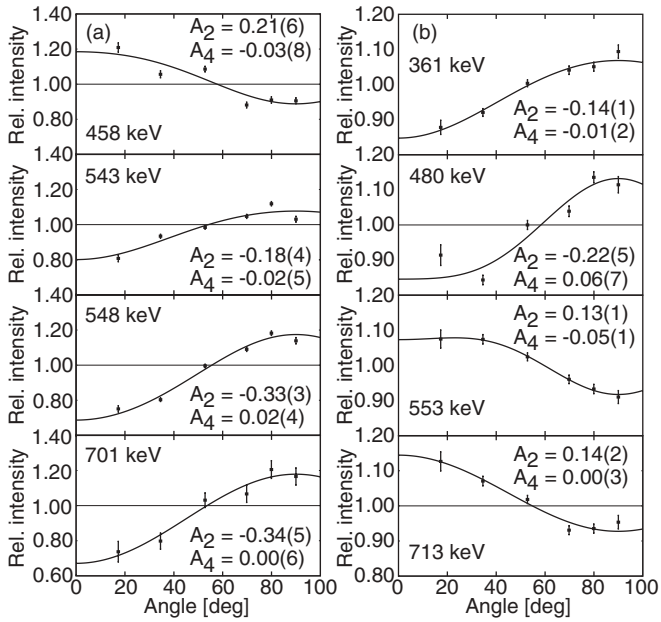

FIG. 4. Angular distributions for known (a) and four new, strong γ rays (b) in ^{206}Bi. Measured points are shown together with the fitted curves and the corresponding A_2 and A_4 coefficients.

resulting from this analysis is then 0.6(1) [10]. A similar analysis carried out for the A_4 coefficient shows that its attenuation is 0.2(6). These attenuation coefficients do not change significantly over the full cascade. Measured A_2 and A_4 coefficients together with deduced δ mixing ratios can be found in Table II for relevant transitions. The other two transitions on the left section of Fig. 4, i.e., the 548- ($14^- \rightarrow 13^-$) and 701- ($18^+ \rightarrow 17^+$) keV lines, are of dominant $M1$ multipolarity. The A_2 coefficient results in the $E2/M1$ mixing ratio δ given in Table II. A second solution of $\delta \sim -5$ would be possible for the measured A_2 value in both cases, but would give too large an A_4 coefficient: 0.11 for both the 548- and 701-keV transitions, clearly outside of the experimental errors. The results of the present analysis for the known 458-, 543-, 548-, and 701-keV transitions in Fig. 4 are in agreement with the multipolarities assigned in the work of Lönnroth *et al.* [1]. From the newly established transitions, only the four with energies of 361, 480, 553, and 713 keV are sufficiently intense to obtain angular distributions (Fig. 4) and provide information on the associated multipolarities. The spin alignment gained in deep-inelastic collisions does not survive the $T_{1/2} > 2$-μs isomer, but the analysis of the angular distributions of prompt γ rays from levels located below this 10 170-keV long-lived state was possible due to the presence of strong prompt side feeding to the levels at 9233, 8520, 8159, and 7679 keV. The 361- and 480-keV lines are characterized by a negative A_2 value and, therefore, are of $\Delta J = 1$ character. The positive A_2 value for the 553-keV line indicates a stretched-$E2$ transition (note that $M2$ or $E3$ possibilities would be isomeric) whereas the 713-keV line below the 155-ns isomer must be of $M2$ or $E3$ character. Mixing ratios for the 361-, 480-, and 713-keV γ rays were derived from their A_2 coefficients, assuming that the 553-keV line is a pure $\Delta J = 2$ $E2$ transition.

III. SPIN-PARITY ASSIGNMENTS

Considering the spin-parity assignments for the newly identified excitations in ^{206}Bi, one has to remember that deep-inelastic reactions strongly favor the population of yrast and near-yrast levels. Thus, level sequences are mostly characterized by a monotonic rise of spin with excitation energy. This consideration provides input complementary to firm experimental information in the form of selection rules, conversion coefficients, and angular distributions. Only $E1$, $M1$, and $E2$ multipolarities were considered for prompt transitions. In addition to the experimental information, the results of shell-model calculations were used to interpret the new levels of ^{206}Bi. The calculations, performed with the OXBASH code [12], allowed one proton particle and three neutron holes relative to ^{208}Pb in the space of $Z \geqslant 82$, $N \leqslant 126$ comprising the orbitals $p_{1/2}$, $p_{3/2}$, $f_{5/2}$, $f_{7/2}$, $h_{9/2}$, and $i_{13/2}$. The single-particle energies were taken from experiment as summarized in Ref. [13]. The residual interaction of Kuo and Herling [14] was used, but with the modifications applied in Refs. [15–17]. In addition, the $\langle \nu i_{13/2}^{-1} | H | \nu i_{13/2}^{-1} \rangle$ matrix elements for J^π 10^+, 12^+ and $\langle \pi i_{13/2} | H | \nu i_{13/2}^{-1} \rangle$ for 12^+, 13^+ have been adjusted to fit the experimental levels [4,5].

The results of the calculations for ^{206}Bi, including only yrast and near-yrast states in the spin range 10–23, are compared with the data in Fig. 1 and Table III. The calculated energies of all low-lying states with $J = 10$–18 agree well with experiment. Above the 18^+ state at 4307 keV, the density of states increases. Nevertheless, there is a clear similarity between the experimental and calculated level structures in the energy range 4.3–7.1 MeV. Only two states, 20_1^+ and 21_1^+ at 6685 and 6872 keV, respectively, stayed without experimental counterparts (Table III). The decay proceeds through many branches, resulting in a rather complex structure in this part of the level scheme. For example, five 19^- states at energies of 5207, 5402, 5610, 5793, and 5882 keV were identified. At 7118 keV, the calculations predict the state with $J^\pi = 23^+$ arising from the maximally-aligned spin coupling of the valence proton particle and three neutron holes, $\pi i_{13/2} \nu i_{13/2}^{-3}$. This calculated state is associated with the experimental level at 7202 keV, that is, with the highest excitation in the 4.3- to 7.2-MeV range. Consequently, a state identified at 7126 keV is a good candidate for the 22^+ excitation. The 76-keV $M1$ transition between these two states is not observed owing to high conversion probability and the low detection efficiency of Gammasphere at this energy. Tentative spin-parity assignments have been proposed for the levels located in this part of the level scheme, that is, between the yrast 18^+ and 23^+ states, based on their decay pattern and the results of shell-model calculations. It is worth noting that all but three of the newly found states have their theoretical counterparts within 80 keV and, except for one level, have the same ordering. The proposed spin-parity assignments are given in Fig. 1 and are listed in Table I. However, it should be emphasized again that the spin assignments rely heavily on comparison with calculation and, in view of the calculated high level density in parts of the spin range, remain tentative.

TABLE III. List of yrast and near-yrast states up to spin $J = 23$ in ^{206}Bi. Spin-parity values, main configurations, and calculated energies are given in the first three columns and compared with experimental energies in the fourth column. The last column provides the probability of the main configuration.

J^π	Main configuration	Calculated energy (keV)	Experimental energy (keV)	Probability of the main configuration (%)
10^-_1	$\pi h_{9/2}\nu p^{-2}_{1/2} i^{-1}_{13/2}$	1084	1045	55.37
11^-_1	$\pi h_{9/2}\nu f^{-1}_{5/2} p^{-1}_{1/2} i^{-1}_{13/2}$	1716	1639	58.00
12^-_1	$\pi h_{9/2}\nu f^{-1}_{5/2} p^{-1}_{1/2} i^{-1}_{13/2}$	1752	1789	75.93
13^-_1	$\pi h_{9/2}\nu f^{-1}_{5/2} p^{-1}_{1/2} i^{-1}_{13/2}$	2065	2056	92.63
13^-_2	$\pi h_{9/2}\nu f^{-2}_{5/2} i^{-1}_{13/2}$	2551	2500	45.72
14^-_1	$\pi h_{9/2}\nu f^{-2}_{5/2} i^{-1}_{13/2}$	2585	2604	85.31
14^-_2	$\pi h_{9/2}\nu f^{-1}_{5/2} p^{-1}_{1/2} i^{-1}_{13/2}$	2971	2951	71.32
15^+_1	$\pi h_{9/2}\nu p^{-1}_{1/2} i^{-2}_{13/2}$	3180	3147	87.57
17^+_1	$\pi h_{9/2}\nu f^{-1}_{5/2} i^{-2}_{13/2}$	3622	3606	97.01
16^+_1	$\pi h_{9/2}\nu f^{-1}_{5/2} i^{-2}_{13/2}$	3675	3652	72.14
18^+_1	$\pi h_{9/2}\nu f^{-1}_{5/2} i^{-2}_{13/2}$	4276	4307	97.48
16^-_1	$\pi h_{9/2}\nu f^{-1}_{7/2} f^{-1}_{5/2} i^{-1}_{13/2}$	4415	4687	89.93
16^-_2	$\pi i_{13/2}\nu p^{-1}_{1/2} i^{-2}_{13/2}$	4844	4775	75.29
17^-_1	$\pi i_{13/2}\nu p^{-1}_{1/2} i^{-2}_{13/2}$	4858	4805	80.53
19^+_1	$\pi h_{9/2}\nu f^{-1}_{5/2} i^{-2}_{13/2}$	4978	4982	98.15
18^-_1	$\pi i_{13/2}\nu p^{-1}_{1/2} i^{-2}_{13/2}$	5041	4993	66.58
18^-_2	$\pi h_{9/2}\nu i^{-3}_{13/2}$	5128	5096	97.26
19^-_1	$\pi i_{13/2}\nu f^{-1}_{5/2} i^{-2}_{13/2}$	5232	5207	49.39
18^-_3	$\pi i_{13/2}\nu f^{-1}_{5/2} i^{-2}_{13/2}$	5334	5278	70.90
18^-_4	$\pi i_{13/2}\nu f^{-1}_{5/2} i^{-2}_{13/2}$	5485	5378	81.13
19^-_2	$\pi i_{13/2}\nu f^{-1}_{5/2} i^{-2}_{13/2}$	5447	5402	51.00
20^-_1	$\pi i_{13/2}\nu f^{-1}_{5/2} i^{-2}_{13/2}$	5541	5511	97.50
19^-_3	$\pi h_{9/2}\nu i^{-3}_{13/2}$	5619	5610	94.03
19^-_4	$\pi i_{13/2}\nu f^{-1}_{5/2} i^{-2}_{13/2}$	5743	5793	97.29
19^-_5	$\pi i_{13/2}\nu f^{-1}_{5/2} i^{-2}_{13/2}$	5941	5882	90.97
21^-_1	$\pi i_{13/2}\nu f^{-1}_{5/2} i^{-2}_{13/2}$	5857	5928	98.62
20^-_2	$\pi i_{13/2}\nu f^{-1}_{5/2} i^{-2}_{13/2}$	5984	5941	94.85
20^-_4	$\pi h_{9/2}\nu i^{-3}_{13/2}$	6272	6349	98.06
19^+_4	$\pi h_{9/2}\nu f^{-1}_{7/2} i^{-2}_{13/2}$	6653	6578	68.84
20^+_1	$\pi h_{9/2}\nu h^{-1}_{9/2} i^{-2}_{13/2}$	6685	–	97.73
19^+_5	$\pi i_{13/2}\nu i^{-3}_{13/2}$	6757	6745	91.39
20^+_2	$\pi h_{9/2}\nu h^{-1}_{9/2} i^{-2}_{13/2}$	6844	6888	90.23
21^+_1	$\pi i_{13/2}\nu i^{-3}_{13/2}$	6872	–	98.87
20^+_3	$\pi i_{13/2}\nu i^{-3}_{13/2}$	6942	6895	88.91
20^+_4	$\pi i_{13/2}\nu i^{-3}_{13/2}$	7007	6990	92.90
21^+_2	$\pi i_{13/2}\nu i^{-3}_{13/2}$	7054	7015	97.29
22^+_1	$\pi i_{13/2}\nu i^{-3}_{13/2}$	7063	7126	100.00
23^+_1	$\pi i_{13/2}\nu i^{-3}_{13/2}$	7118	7202	100.00

The levels located above the 7202-keV state with $J > 23$ have to originate from neutron and/or proton excitations across the $N = 126$ and $Z = 82$ shell gaps, respectively. As the decay of the isomeric state at 9233 keV proceeds mostly through a single cascade, the intensities of γ rays belonging to this 713-, 361-, 480-, and 553-keV sequence are sufficiently strong to deduce their angular distributions and conversion coefficients. As stated earlier, the angular distribution (Fig. 4) and conversion coefficient (Table II) for the 553-keV γ ray uniquely point to its stretched-$E2$ character. Assuming that this transition directly feeds the 22^+ state, a spin-parity of 24^+ can be assigned to the 7679-keV level. In turn, results of a similar

analysis for the 480- and 361-keV lines (negative A_2 and conversion coefficients of 0.18(4) and 0.26(2), respectively), are compatible with their $M1$ and $\Delta J = 1$ character. This results in respective quantum number assignments of 25^+ and 26^+ for the 8159- and 8520-keV states.

It should be acknowledged, however, that one cannot definitely rule out that all three 480-553, 477-76, and 346-568-keV branches feed the 23^+ state which then in turn would decay to the 22^+ level by a low-energy, $E_\gamma < 80$ keV, unobserved $M1$ transition. In such a scenario, the ordering of the 76-keV γ ray in the cascade would be uncertain as well. Furthermore, the spin assignments for the core-excited states, described below, would change and all the values would be larger by $1\hbar$.

Next, for the 713-keV transition deexciting the 155-ns isomer, the angular distribution limits the spin change ΔJ to 2 or 3, whereas the conversion coefficient, 0.10(3), clearly indicates an $M2$ character. Therefore, 28^- quantum numbers are assigned to the isomer at 9233 keV.

An analysis of the angular distribution or conversion coefficient for the 937-keV line connecting the two isomers could not be performed. However, by considering that the half-life of the 10 170-keV isomer is significantly longer than 2 μs and by taking into account the half-lives of isomers existing in this region of the nuclear chart, an assignment of $E3$ multipolarity to the 937-keV γ ray would appear to be most probable. It follows then that the 10 170-keV level would have tentative $J^\pi = 31^+$ quantum numbers.

IV. DISCUSSION

Because of remarkably large energy gaps separating both proton and neutron shells at $Z = 82$ and $N = 126$, respectively, the ^{208}Pb nucleus is often considered to be one of the best doubly-magic nuclei in nature. As a result, nuclei located in its immediate vicinity are usually described rather well within the shell model (SM). With a single proton particle and three neutron holes outside ^{208}Pb, the ^{206}Bi nucleus belongs to this category of "shell model nuclei" and its yrast structure is expected to be described well in terms of valence particle-hole couplings computed within this SM framework. As indicated above, the spin-parity assignments to states within the 4- to 7-MeV excitation range in ^{206}Bi were heavily based on comparisons with SM results. Hence, the choice of an interaction providing reliable predictions in this instance becomes important. In the present study, an improved version of the Kuo-Herling interaction [14] was selected in view of its success in describing recent, extensive results in ^{205,204}Pb [18,19], ^{208}Bi [5], ^{203}Hg [4], and ^{204}Tl [3].

As can be seen from Fig. 1, the lower part of the ^{206}Bi level scheme up to the 18^+ level at 4.3 MeV, where spin-parity assignments are firm, is described well by the calculations, inspiring confidence in their ability to account for the higher excitations. Indeed, the experimental ground-state binding energy of 18.645(8) MeV relative to ^{208}Pb is calculated to be 18.685 MeV reproducing it to within 40 keV. The success of the calculations can also be realized from the fact that the well-established 22^+ state at the high end of the spin-energy range under consideration has a calculated binding energy within 63 keV of experiment (see Table III).

In the 4.3- to 7.1-MeV range, the yrast and near-yrast structures are rather complex with a large number of states and a multitude of decay paths. Despite this apparent complexity, the comparison between the newly-established data and the calculations in this range is rather striking and the agreement is satisfactory.

The following general features can be highlighted from comparisons between experiment and calculations. The states immediately above the 10^- isomer are characterized by a negative parity and are understood as arising from excitations involving a proton particle occupying the $h_{9/2}$ orbital while the neutron holes occupy the opposite parity $f_{5/2}$, $p_{1/2}$, and $i_{13/2}$ states. Moving up in excitation energy above the 14^- levels, a parity change occurs and the dominant sequence takes place between the 15.6-ns, 15^+ isomer and the 19^+ level at 4982 keV. As seen in Table III, the calculations indicate that these states involve the dominant $\pi h_{9/2}\nu f_{5/2}^{-1} i_{13/2}^{-2}$ configuration, with the exception of the 3147-keV, 15^+ level with a dominant $\pi h_{9/2}\nu p_{1/2}^{-1} i_{13/2}^{-2}$ component in its wave function; i.e., the $f_{5/2}$ neutron hole is being replaced by the $p_{1/2}$ one located close in excitation energy. Starting from an energy of $\sim$4.6 MeV, most of the states are of negative parity, an observation accounted for in the calculations by the proton occupying preferentially the $i_{13/2}$ orbital while two neutron holes are in the corresponding $i_{13/2}$ state with the third occupying either the $p_{1/2}$ or $f_{5/2}$ state. The members of the $\pi i_{13/2}\nu f_{5/2}^{-1} i_{13/2}^{-2}$ multiplet "terminate" in a calculated 5857-keV 21^- state resulting from the maximal alignment of all spins in this configuration. The associated experimental level is located 71 keV higher, at 5928 keV. For the highest valence excitations, above $\sim$6.7 MeV, another change in parity is observed and the levels have a $\pi i_{13/2}\nu i_{13/2}^{-3}$ main configuration, which terminates in a maximally-aligned, "terminating" 23^+ state computed at 7118 keV and associated with the 7202-keV level in the data.

Of particular interest are the two isomers located at 9233 (with the half-life $T_{1/2} = 155$ ns) and 10170 keV ($T_{1/2} > 2$ μs) with probable spin-parity 28^- and 31^+. The second of these belongs to a very restricted group of states with lifetimes of one microsecond or longer that have such a high spin. It is quite certain that these two isomeric states, as well as other yrast excitations located above spin 23^+ in ^{206}Bi, have to involve excitations across the shell gaps at $N = 126$ and/or $Z = 82$; that is, core excitations. There is, however, no obvious guidance about which of the low-lying states in ^{206}Bi and which of the core excitations in ^{208}Pb would couple to give rise to isomers. Indeed, such couplings on the one hand involve one-proton-particle and three-neutron-holes configurations and, on the other, neutron or proton particle-hole excitations which are too complex to evaluate excitation energies from first principles. To describe these levels, the appropriate SM calculations would have to be carried out, but these are presently difficult to perform owing to limitations imposed by the large model space. Thus, the levels located in ^{206}Bi above spin 23^+, can serve as a suitable testing ground

for future large SM calculations that involve particle-hole excitations near doubly magic ^{208}Pb.

V. SUMMARY

Extensive γ-ray coincidence data acquired with Gammasphere for the system ^{76}Ge + ^{208}Pb have provided much information about yrast and near-yrast excitations in ^{206}Bi, above the previously established 10^- isomer. Angular distributions of γ rays from the spin-aligned states in ^{206}Bi products were instrumental in proposing spin-parity assignments. The interpretation of medium-energy ^{206}Bi excitations was facilitated by detailed comparisons with results from SM calculations performed with a recently developed empirical interaction. States identified at energies up to about 7 MeV can be described satisfactorily in terms of one-proton-particle, three-neutron-hole couplings.

The new findings include two high-spin isomers arising from ^{208}Pb core excitations. Spin-parity values of 31^+ have been tentatively assigned to a microsecond isomer located at 10 170 keV, the state with the highest spin observed in deep-inelastic reaction studies and with one of the longest lifetimes known at a spin above $30\hbar$.

ACKNOWLEDGMENTS

The authors thank the ATLAS operating staff for the efficient running of the accelerators and John Greene for preparing the target used in the measurement. This work is supported by the National Science Centre under Contract No. DEC-2011/01/N/ST2/04612, by the Polish Ministry of Science and Higher Education under Contract No. N-N202-263238, and by the US Department of Energy, Office of Nuclear Physics, under Contracts No. DE-AC02-06CH11357 and No. DE-FG02-94ER40834.

[1] T. Lönnroth, L. Végh, K. Wikström, and B. Fant, Z. Phys. A **287**, 307 (1978).
[2] J. Wrzesiński *et al.*, Eur. Phys. J. A **20**, 57 (2004).
[3] R. Broda *et al.*, Phys. Rev. C **84**, 014330 (2011).
[4] B. Szpak *et al.*, Phys. Rev. C **83**, 064315 (2011).
[5] B. Fornal *et al.*, Phys. Rev. C **67**, 034318 (2003).
[6] B. Fornal *et al.*, Phys. Rev. Lett. **87**, 212501 (2001).
[7] R. Broda, J. Phys. G **32**, R151 (2006).
[8] I.-Y. Lee, Nucl. Phys. A **520**, 641c (1990).
[9] F. G. Kondev, Nucl. Data Sheets **109**, 1527 (2008).
[10] T. Yamazaki, Nucl. Data A **3**, 1 (1967).
[11] H. Morinaga and T. Yamazaki, *In-beam Gamma-ray Spectroscopy* (North-Holland, Amsterdam, 1976).
[12] B. A. Brown, A. Etchegoyen, N. S. Godwin, W. D. M. Rae, W. A. Richter, W. E. Ormand, E. K. Warburton, J. S. Winfield, L. Zhao, and C. H. Zimmerman, MSU-NSCL Report No. 1289 (unpublished).
[13] M. Rejmund, M. Schramm, and K. H. Maier, Phys. Rev. C **59**, 2520 (1999).
[14] T. T. S. Kuo and G. Herling, US Naval Research Laboratory Report No. 2258, 1971 (unpublished); G. Herling and T. T. S. Kuo, Nucl. Phys. A **181**, 113 (1972).
[15] L. Rydström, J. Blomqvist, R. J. Liotta, and C. Pomar, Nucl. Phys. A **512**, 217 (1990).
[16] J. B. McGrory and T. T. S. Kuo, Nucl. Phys. A **247**, 283 (1975).
[17] K. H. Maier *et al.*, Phys. Rev. C **76**, 064304 (2007).
[18] F. G. Kondev, Nucl. Data Sheets **101**, 521 (2004).
[19] C. J. Chiara and F. G. Kondev, Nucl. Data Sheets **111**, 141 (2010).